Am J Clin Exp Immunol 2024;13(1):12-25
www.ajcei.us /ISSN:2164-7712/AJCEI0154431

Original Article

Identification of glycosyltransferase-related genes signature and integrative analyses in patients with ovarian cancer

Yanqiu Zhang[1,2], Tong Zhou[1,3], Qingqin Tang[1], Bin Feng[1], Yuting Liang[1]

[1]Center for Clinical Laboratory, The First Affiliated Hospital of Soochow University, Suzhou, Jiangsu, The People's Republic of China; [2]Institute of Clinical Pharmacology, Anhui Medical University, Key Laboratory of Anti-inflammatory and Immune Medicine, Ministry of Education, Anhui Collaborative Innovation Center of Anti-inflammatory and Immune Medicine, Hefei, Anhui, The People's Republic of China; [3]Medical College of Soochow University, Suzhou, Jiangsu, The People's Republic of China

Received November 15, 2023; Accepted February 19, 2024; Epub February 25, 2024; Published February 28, 2024

Abstract: Background: Glycosyltransferases (GT) play a crucial role in glycosylation reactions, and aberrant expression of glycosyltransferase-related genes (GTs) leads to abnormal glycosylation, which is associated with tumor progression. However, the prognostic value of aberrant expression of GTs in ovarian cancer (OC) and the correlation between GTs and tumor microenvironment (TME) remain unknown. Methods: TCGA and GSE53963 databases were used to obtain data on OC patient samples. The association of GTs with OC was analyzed. Molecular subtypes were identified by consensus unsupervised clustering, followed by immune infiltration and functional enrichment analyses. Survival analysis was performed using Kaplan-Meier curves and log-rank tests. Least Absolute Shrinkage and Selection Operator (LASSO) and multifactorial cox regression were used to screen for signature genes associated with OC and used to establish prognostic models. Result: OC patients were categorized into 5 GTs clusters using consensus unsupervised cluster analysis. Clusters D and E showed significant differences between survival, signaling pathways and immune infiltration. Then, a risk model was developed based on the 12 signature genes, which provides a more accurate evaluation of the prognosis of OC patients. We categorized patients into high-risk and low-risk groups based on the risk score and found that the survival of patients in the high-risk group was significantly lower than that in the low-risk group. Moreover, the risk score was significantly correlated with tumor microenvironment, immune infiltration, and chemotherapy sensitivity. Conclusion: Overall, we performed a comprehensive analysis of GTs in OC patients and developed a risk model for OC. Our findings will provide a new insight to OC prognosis and treatment.

Keywords: Glycosyltransferase, ovarian cancer, tumor microenvironment, immune cell infiltration

Introduction

Ovarian cancer (OC) is one of the most common and lethal malignancy among gynecological tumors with an incidence of 3.4% and a mortality rate of 4.7% [1, 2]. Characterized by late presentation and poor prognosis, OC poses a significant challenge [3, 4]. This challenge is mainly due to the lack of specific biomarkers and early effective screening tools, resulting in more than 70% of patients not being diagnosed until advanced stages [5, 6]. Despite the implementation of various therapeutic strategies such as chemotherapy, radiotherapy and immunotherapy, the survival rates of OC patients have shown limited improvement [7]. Therefore, the identification of reliable prognostic biomarkers for OC patients is of paramount importance to improve survival and prognosis.

Glycosylation is a common process for modifying lipids and proteins, catalyzed primarily by glycosyltransferases (GT) to produce various glycoconjugates. These glycoconjugates are actively involved in various biological processes, including cell growth, adhesion, signal transduction, and immune response [8, 9]. Abnormal glycosylation, on the other hand, is associated with numerous pathologies, such as cancer, viral infections, and autoimmune diseases, and

is recognized as a hallmark of tumors [10]. GT, a large family of enzymes located in the endoplasmic reticulum and Golgi apparatus, play a crucial role in the glycosylation process [8]. Accumulating evidence indicates that aberrant expression of glycosyltransferase-related genes (GTs) directly influences tumorigenesis, progression and chemotherapy resistance [11]. Despite the abundance of studies on GTs in various contexts, there is a notable lack of research focusing on GTs in OC. Therefore, further investigation is essential to elucidate the specific mechanisms involved.

In this study, we evaluated the diagnostic, prognostic, and therapeutic potential of GTs in OC. Risk scores were constructed based on differential genes associated with prognosis by molecular typing, which showed high accuracy in predicting clinical prognosis, immune infiltration, and pharmacotherapeutic response.

Materials and methods

Data acquisition

Gene expression profiles and corresponding clinical information of OC samples were obtained from The Cancer Genome Atlas (TCGA) and GSE53963. We extracted 185 GTs based on previous research [12]. Subsequent analysis was conducted using R software (version 4.3.1).

Cluster and principal component analysis (PCA)

According to the expression levels of GTs, we performed an unsupervised cluster analysis using the R package "ConsensusClusterPlus" to categorize OC patients into different glycosyltransferase-related clusters (GTs clusters) [13]. In addition, based on the expression of typing-related genes and cluster data of OC patients, PCA was performed using the R package (limma, ggplot2).

Functional enrichment analysis

The cluster data of OC patients were obtained from cluster analysis. R package "GSVA" was utilized for gene set variation analysis (GSVA), performed with "c2.cp.kegg.symbols" and "c5.go.symbols", and heatmaps of GSVA were plotted using R software. Gene Ontology (GO) and Kyoto Encyclopedia of Genes and Genomes (KEGG) enrichment analyses were performed by R packages (clusterProfiler, org.Hs.eg.db, enrichplot, ggplot2) [14].

Immune cell infiltration analysis

The degree of immune infiltration of immune cells in OC Tumor microenvironment (TME) was quantified using single-sample gene-set enrichment analysis (ssGSEA) in the "GSVA" package [15].

Prognostic risk model construction

Prognostic risk models were constructed using the R packages (survival, caret, glmnet, survminer, and timeROC). The Least Absolute Shrinkage and Selection Operator (LASSO) was applied to screen signature genes for the construction of the prognostic risk model. OC patients were randomly assigned to training and test groups. Prognostic risk scores, derived from gene expression and correlation coefficients, categorized patients into high-risk and low-risk groups based on the median risk score. Kaplan-Meier analysis was used to compare the probability of survival between the two groups, and a Receiver Operating Characteristic (ROC) curve was plotted using "timeROC" R package.

TME, immune infiltration, and chemotherapeutic sensitivity

TME scores for each OC sample were assessed using the R package (ESTIMATE) [16]. The R software package (CIBERSORT) was used to analyze the immune cell infiltration states [17]. Additionally, the R packages (limma, ggplot2, and ggpubr) were employed to calculate the IC50 of the chemistries and compare differences between the two groups.

Statistical analysis

Statistical analyses were analyzed with RStudio and Perl. Survival analysis was performed using the Kaplan-Meier method, and significance of differences was determined by the log-rank test. Group comparisons were conducted using the Wilcoxon test, with $P<0.05$ considered statistically significant.

Result

Genetic and transcriptional variations of GTs in OC

Based on published articles, we obtained a list of 185 GTs [12]. Subsequently, the expression

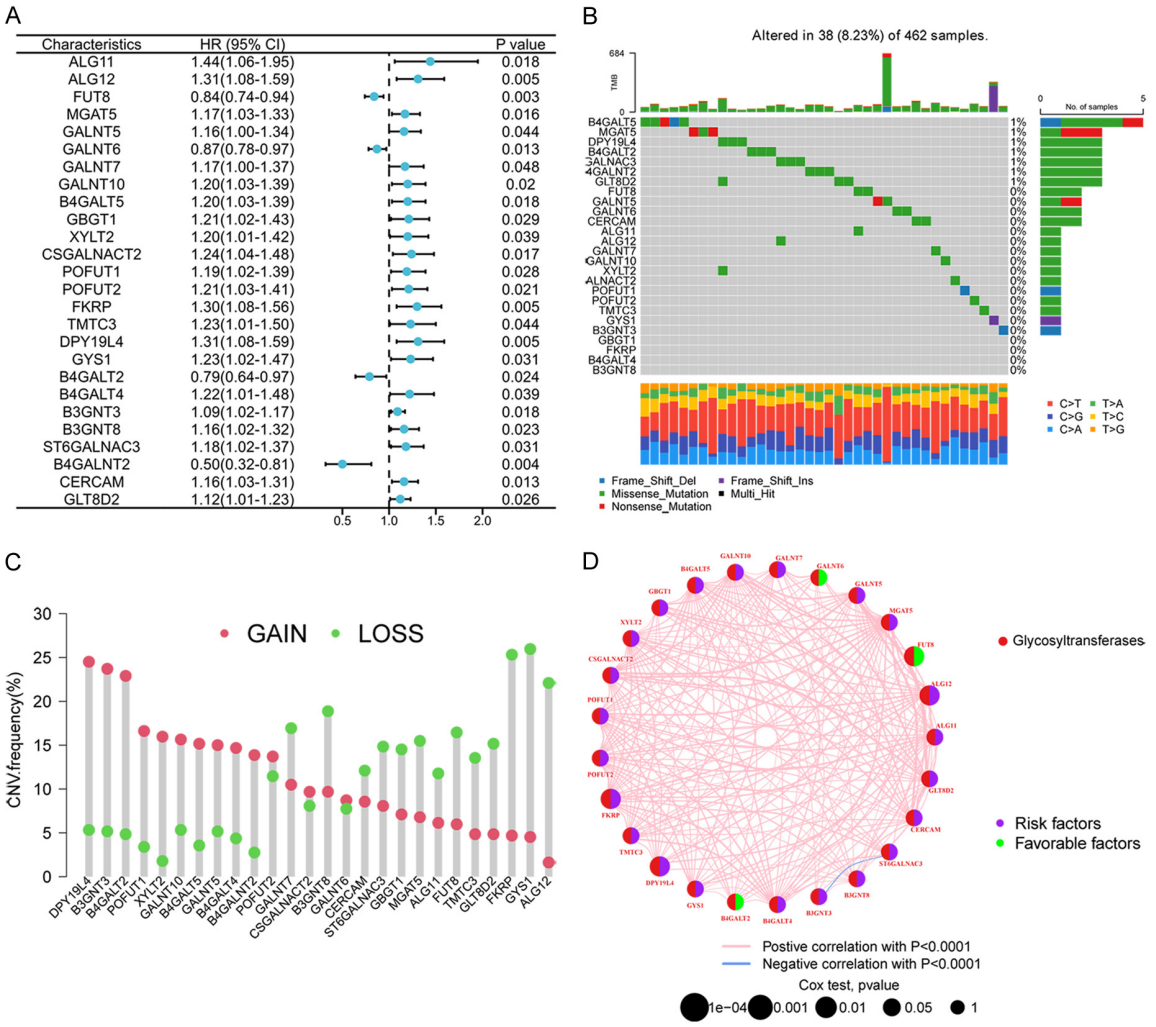

Figure 1. Summary of genetic and transcriptional variations of GTs in OC. A. Univariate cox analysis of 26 GTs associated with HR in patients with OC. B. Genetic variants of 462 OC patients in TCGA cohort. C. CNV amplifications and deletions in GTs in OC patients. D. Network diagram reveals interactions between GTs in OC.

levels of GTs in OC were evaluated using the TCGA database. Among them, 163 GTs exhibited differential expression, initially suggesting abnormal regulation of GTs in OC. To further confirm the relationship between the 163 GTs and OC, the GSE53963 and TCGA datasets were merged to analyze the correlation between the 163 GTs and the hazard ratio (HR) of OC patients, and 26 GTs associated with HR were identified by univariate cox analysis (**Figure 1A**). The mutation status of these genes in OC patients is illustrated in the waterfall plot (**Figure 1B**), with a mutation frequency of 8.23% (38 out of 462 samples) in the TCGA dataset. Among these mutations, B4GALT5 had the highest mutation frequency (1%). Next, we examined the Copy number variation (CNV) frequencies of 26 GTs (**Figure 1C**). We found that DPY19L4 displayed the highest increase in CNV, while GYS1 had the highest deletion. Prognostic network diagram reveals the relevance of GTs to OC prognosis (**Figure 1D**).

Cluster analysis and PCA

According to GTs expression, OC patients were categorized into 5 subtypes via unsupervised consensus clustering (**Figure 2A**). PCA results distinctly illustrated the demarcation between GTs clusters D and E (**Figure 2B**). To elucidate the functional disparities between GTs clusters D and E, GO and KEGG enrichment analyses were performed using GSVA for GTs clusters D and E. The GSVA results revealed that GTs cluster E exhibited notable enrichment in transport-related processes (including Golgi vesicle

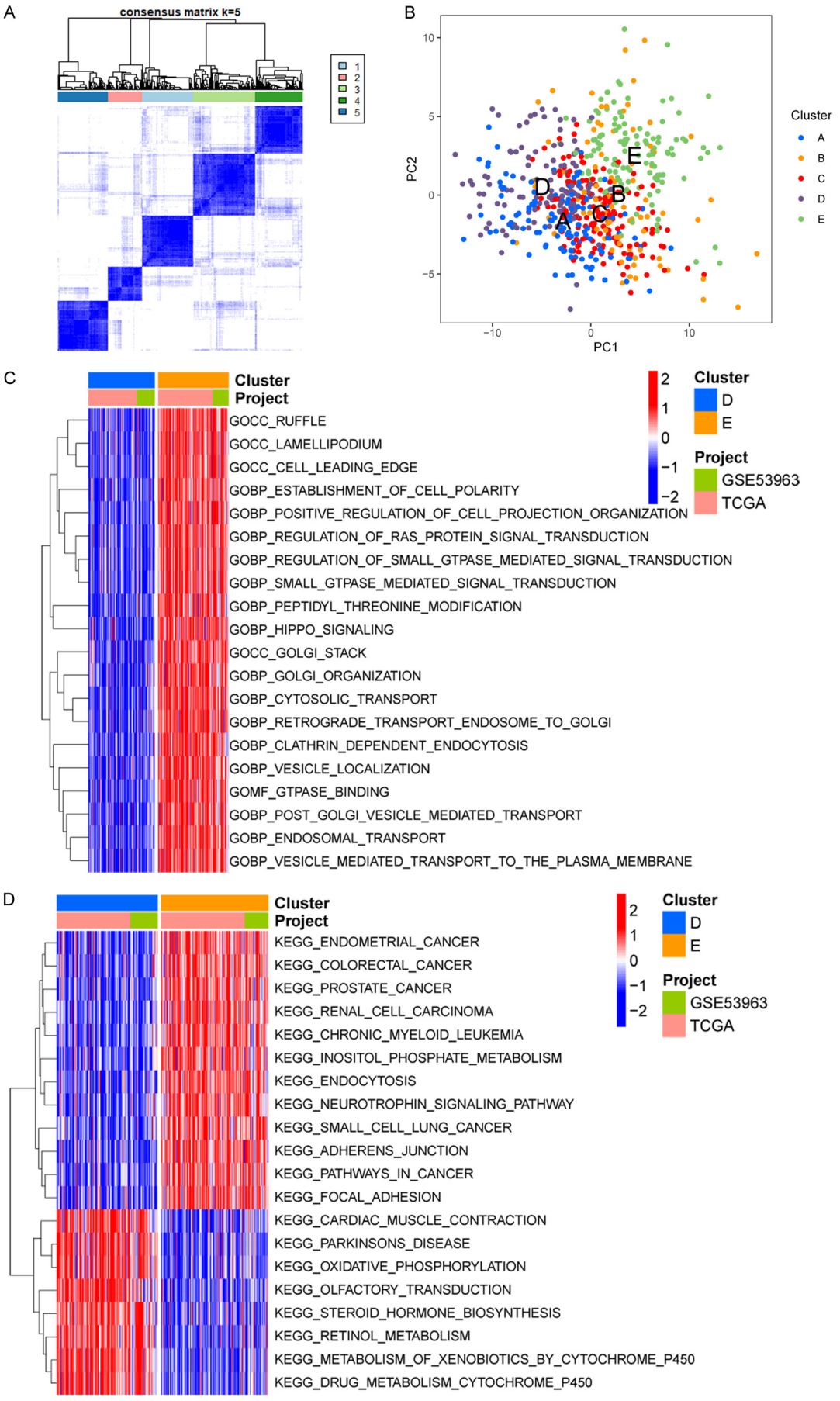
A
consensus matrix k=5
1
2
3
4
5
B
PC2
PC1
Cluster
A
B
C
D
E
C
Cluster
Project
GOCC_RUFFLE
GOCC_LAMELLIPODIUM
GOCC_CELL_LEADING_EDGE
GOBP_ESTABLISHMENT_OF_CELL_POLARITY
GOBP_POSITIVE_REGULATION_OF_CELL_PROJECTION_ORGANIZATION
GOBP_REGULATION_OF_RAS_PROTEIN_SIGNAL_TRANSDUCTION
GOBP_REGULATION_OF_SMALL_GTPASE_MEDIATED_SIGNAL_TRANSDUCTION
GOBP_SMALL_GTPASE_MEDIATED_SIGNAL_TRANSDUCTION
GOBP_PEPTIDYL_THREONINE_MODIFICATION
GOBP_HIPPO_SIGNALING
GOCC_GOLGI_STACK
GOBP_GOLGI_ORGANIZATION
GOBP_CYTOSOLIC_TRANSPORT
GOBP_RETROGRADE_TRANSPORT_ENDOSOME_TO_GOLGI
GOBP_CLATHRIN_DEPENDENT_ENDOCYTOSIS
GOBP_VESICLE_LOCALIZATION
GOMF_GTPASE_BINDING
GOBP_POST_GOLGI_VESICLE_MEDIATED_TRANSPORT
GOBP_ENDOSOMAL_TRANSPORT
GOBP_VESICLE_MEDIATED_TRANSPORT_TO_THE_PLASMA_MEMBRANE
Cluster
D
E
Project
GSE53963
TCGA
D
Cluster
Project
KEGG_ENDOMETRIAL_CANCER
KEGG_COLORECTAL_CANCER
KEGG_PROSTATE_CANCER
KEGG_RENAL_CELL_CARCINOMA
KEGG_CHRONIC_MYELOID_LEUKEMIA
KEGG_INOSITOL_PHOSPHATE_METABOLISM
KEGG_ENDOCYTOSIS
KEGG_NEUROTROPHIN_SIGNALING_PATHWAY
KEGG_SMALL_CELL_LUNG_CANCER
KEGG_ADHERENS_JUNCTION
KEGG_PATHWAYS_IN_CANCER
KEGG_FOCAL_ADHESION
KEGG_CARDIAC_MUSCLE_CONTRACTION
KEGG_PARKINSONS_DISEASE
KEGG_OXIDATIVE_PHOSPHORYLATION
KEGG_OLFACTORY_TRANSDUCTION
KEGG_STEROID_HORMONE_BIOSYNTHESIS
KEGG_RETINOL_METABOLISM
KEGG_METABOLISM_OF_XENOBIOTICS_BY_CYTOCHROME_P450
KEGG_DRUG_METABOLISM_CYTOCHROME_P450
Cluster
D
E
Project
GSE53963
TCGA

Figure 2. Cluster analysis and functional enrichment of DEGs among GTs clusters. A. Cluster analysis categorized OC patients into five clusters (k=5) based on the transcriptome of GTs. B. PCA revealed a clear demarcation between GTs clusters D and E. C, D. GSVA showed significant differences in GO and KEGG pathway enrichment between GTs clusters D and E.

transport and vesicle targeting, etc.) and cancer-associated pathways (including endometrial, colorectal, prostate, and renal carcinomas, etc.) compared to GTs cluster D (**Figure 2C**, **2D**). In addition, 2431 differentially expressed genes (DEGs) were selected between GTs clusters D and E. Subsequently, the physiological functions and pathways affected by these DEGs were analyzed by GO analysis and KEGG analysis (**Figure 3A**, **3B**). The results highlighted the significant regulation of immune-related processes and pathways, including PI3K-AKT signaling pathway and MAPK signaling pathway. To further explore the immune landscape, ssGSEA was performed to assess immune cell infiltration in GTs clusters D and E. The results indicated significant differences between the two clusters (**Figure 3C**). Cluster E displayed lower levels of activated CD4 T cells, activated CD8 T cells, CD56bright natural killer cells, and type 17 T helper cells, while macrophages, mast cells, natural killer cells, neutrophils and eosinophilic T cells, follicular helper cells, and type 1 T helper cells showed higher levels.

Identification of GTs gene clusters in OC and construction of GTs prognostic model

Univariate Cox regression analysis was utilized to assess the prognostic value of 2431 DEGs associated with GTs cluster D and cluster E, and finally 666 DEGs associated with overall survival (OS) were screened (P<0.05). On the basis of the expression levels of OS-related DEGs, OC patients were categorized into three gene clusters using a consensus clustering algorithm (**Figure 4A**). Via Kaplan-Meier analysis, it was confirmed that patients in gene cluster C exhibited a worse prognosis than those in gene clusters A, B (P<0.001) (**Figure 4B**). After that, we constructed a prognostic risk model by screening 12 characterized genes using Lasso (KCTD20, VANGL1, BLOC1S1, VSIG4, WNT11, FAM102A, EPHA4, LYVE1, TMEM181, NSF, SUSD5, and ZNF12) (**Figure 4C-E**). Then we investigated the relationship between GTs clusters and gene clusters with prognostic model risk scores, and we found that GTs cluster E and DEGs cluster C had higher risk scores (**Figure 4F**, **4G**). Finally, we found that high-risk patients had higher expression in 26 GTs (**Figure 4H**). Additionally, by analyzing the three cohorts (all, training and test), we observed that high-risk patients were associated with more deaths and shorter survival times, and the heatmap displayed the differential expression of 12 prognostic signature genes between the high-risk and low-risk groups in the three cohorts (**Figure 5A-C**). The Kaplan-Meier survival analyses demonstrated that, compared to the low-risk group, the high-risk group of patients had a worse survival time (**Figure 5D-F**). ROC curves revealed 1-, 3-, and 5-year AUC values for all group (0.631, 0.653, 0.731), training group (0.679, 0.705, 0.795), and test group (0.591, 0.599, 0.636), respectively (**Figure 5G-I**).

TME, immune infiltration, and chemotherapeutic sensitivity

Next, we explored the mutation burden within the prognostic risk model, and the mutation waterfall plot showed that there was no significant difference in the proportion of mutations between the high- and low-risk groups (**Figure 6A**, **6B**). To further elucidate the relationship between the prognostic risk model and TME scores along with immune cell infiltration, we examined TME scores, which indicated higher stromal scores and estimated scores in the high-risk group (**Figure 6C**). Furthermore, we evaluated the links between immune infiltration with 12 signature genes and risk scores. The results revealed that resting CD4 memory T cells, monocytes, activated mast cells, M0 macrophages, and naive B cells were positively linked to the risk score, whereas follicular helper T cells, CD8 T cells, activated CD4 memory T cells, activated NK cells, M1 macrophages, activated dendritic cells, and memory B cells were negatively linked to the risk score (**Figures 6D**, S1). Later, through drug sensitivity analysis, we observed that high-risk patients had lower IC50 for Cediranib, Dasatinib, Foreinib, and AZD8186, while low-risk patients had lower IC50 for cisplatin and Niraparib (**Figure 6E**).

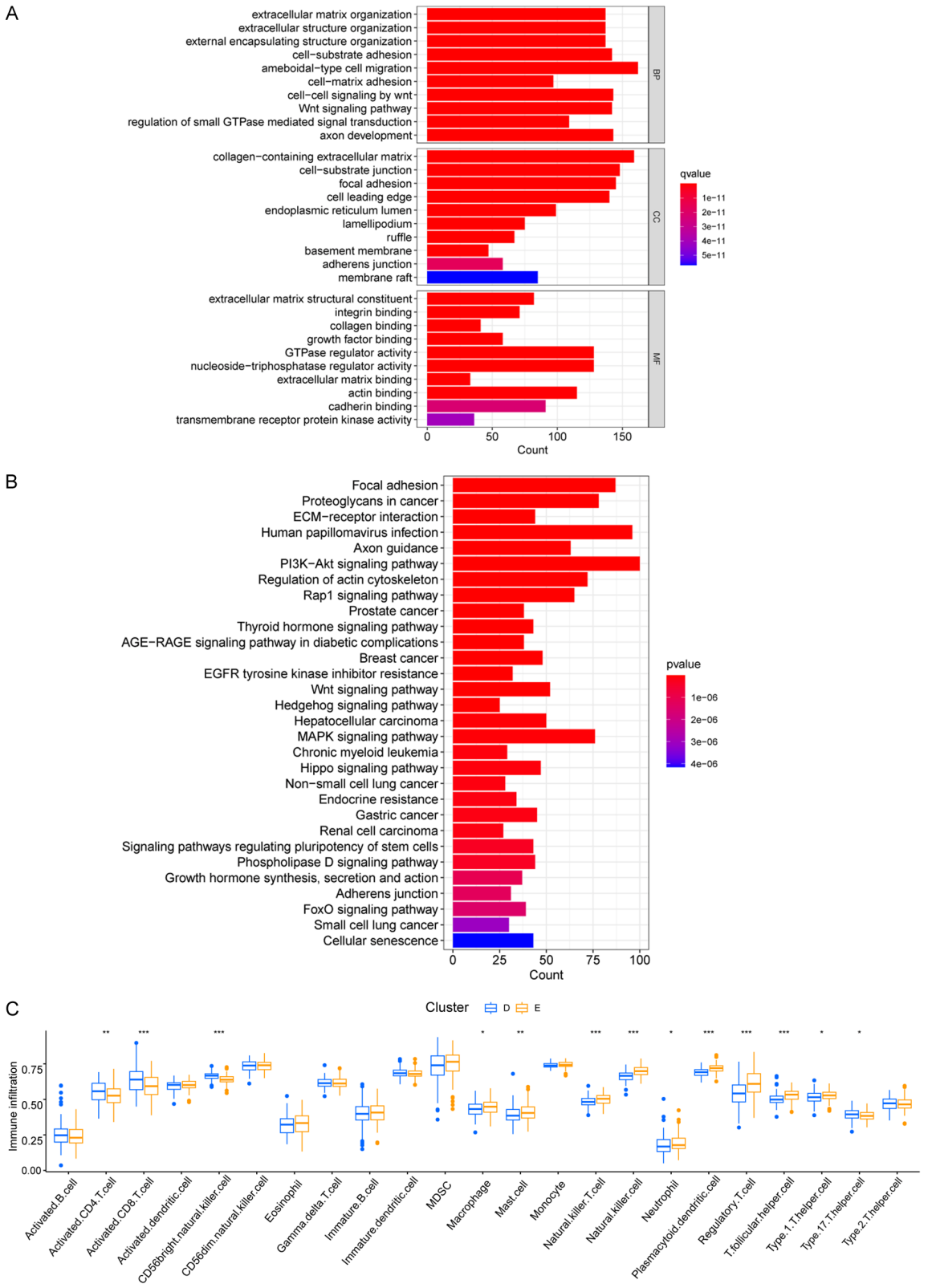

Figure 3. Function analysis and immune cell infiltration. A, B. GO analysis and KEGG analysis illuminated physiological functions and pathways influenced by DEGs between GTs clusters D and E. C. Correlation between immune cell infiltration with GTs clusters.

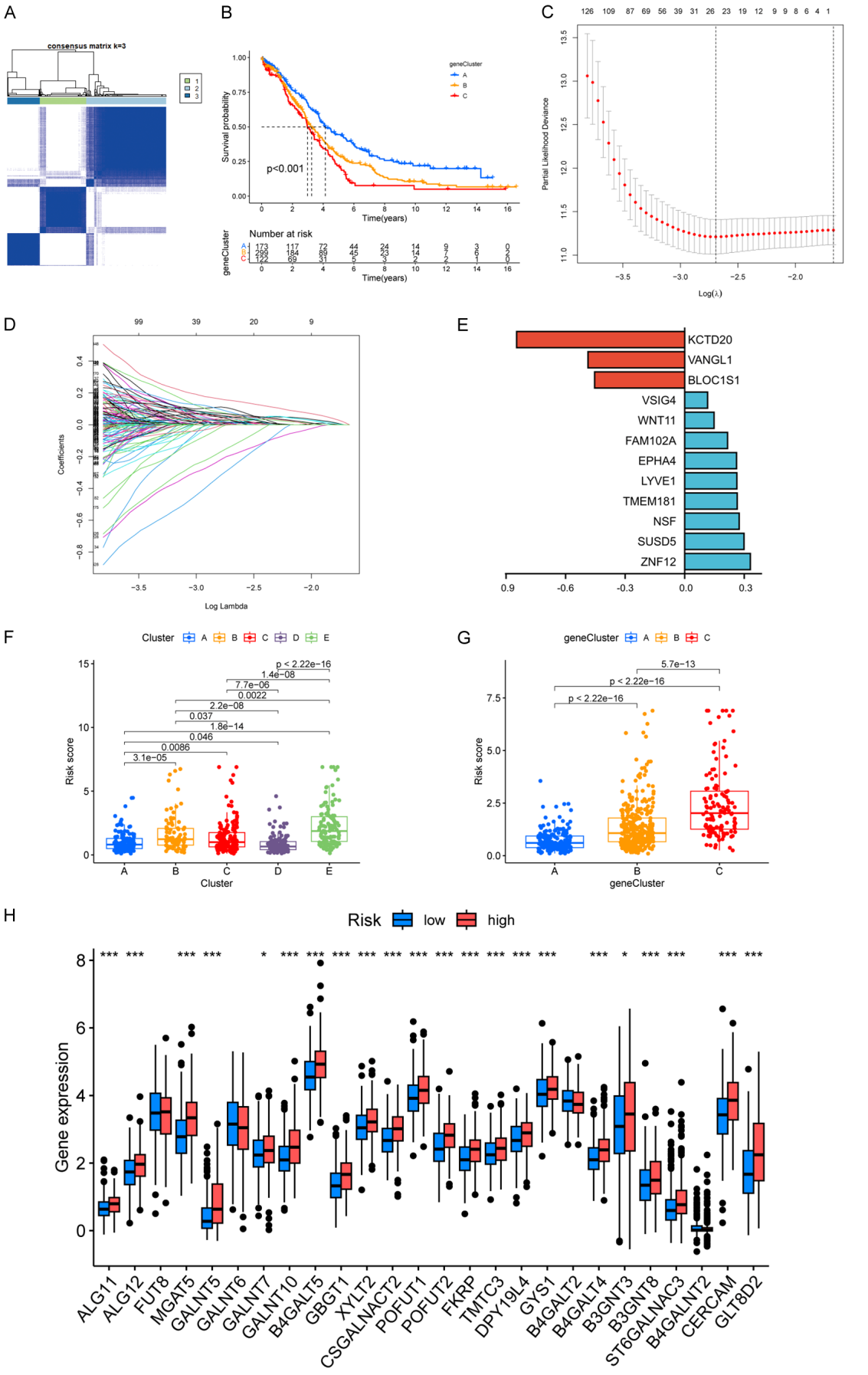
A
consensus matrix k=3
B
Survival probability
p<0.001
Time(years)
geneCluster
Number at risk
C
Partial Likelihood Deviance
Log(λ)
D
Coefficients
Log Lambda
E
KCTD20
VANGL1
BLOC1S1
VSIG4
WNT11
FAM102A
EPHA4
LYVE1
TMEM181
NSF
SUSD5
ZNF12
F
Cluster
Risk score
p < 2.22e−16
1.4e−08
7.7e−06
0.0022
2.2e−08
0.037
1.8e−14
0.046
0.0086
3.1e−05
G
geneCluster
Risk score
5.7e−13
p < 2.22e−16
p < 2.22e−16
H
Risk low high
Gene expression
ALG11
ALG12
FUT8
MGAT5
GALNT5
GALNT6
GALNT7
GALNT10
B4GALT5
GBGT1
XYLT2
CSGALNACT2
POFUT1
POFUT2
FKRP
TMTC3
DPY19L4
GYS1
B4GALT2
B4GALT4
B3GNT3
B3GNT8
ST6GALNAC3
B4GALNT2
CERCAM
GLT8D2

Figure 4. Identification of gene clusters and construction of OC prognostic models. A. OC patients were categorized into 3 gene clusters (k=3) according to the expression of OS related DEGs. B. Kaplan-Meier survival curves for OC patients in the three gene clusters. C-E. LASSO analysis and multivariate Cox regression analysis screened for 12 signature genes. F. Differences in risk scores between GTs cluster A to E. G. Differences in risk scores between gene cluster A and C. H. Differences in the expression levels of 26 GTs between high-risk and low-risk groups. *P*-values were shown as: *P<0.05; **P<0.01; ***P<0.001.

Discussion

OC is a severe disease associated with high morbidity and mortality rates, posing a serious threat to women's health. Abnormal glycosylation, recognized as a cancer marker, has garnered increasing attention, offering a novel perspective for the prognosis and treatment of OC [8]. Abnormal glycosylation mainly caused by abnormal expression of GT. Given the limited understanding of the role of GTs in OC, this study employed various machine learning algorithms to investigate their impact. Prognostic signature genes were meticulously screened to establish an OC risk model, and the accuracy of this model was rigorously evaluated through considerations of immune infiltration, tumor microenvironment scores, and sensitivity to chemotherapeutic drugs.

OC patients were stratified into 5 clusters based on the distinct gene expression patterns of GTs (**Figure 2A**). Subsequent analyses, including PCA, GSVA, GO, KEGG revealed significant differences between Clusters D and E, with cluster D exhibiting a worse prognosis (**Figures 2**, **3**). Following DEGs clustering, LASSO regression, and Cox multifactorial analysis, a prognostic risk model consisting of 12 genes (KCTD20, VANGL1, BLOC1S1, VSIG4, WNT11, FAM102A, EPHA4, LYVE1, TMEM181, NSF, SUSD5, and ZNF12) was constructed (**Figure 4C-E**). Among these signature genes, VSIG4, a novel member of the immunoglobulin superfamily, showed specific expression in tissue macrophages. While it enhanced macrophage phagocytosis and maintained immune homeostasis, its immunosuppressive role in the microenvironment contributed to tumor progression [18, 19]. Recent studies have also implicated VSIG4 in the modulation of OC cell proliferation and migration [19]. Another notable gene, WNT11, a non-canonical member of the Wnt family, played a pivotal role in tumor progression by promoting proliferation, invasion and metastasis in various cancers, including ovarian [20], breast [21] and colorectal cancers [22]. Similarly, high expression of EPHA4 promotes tumor progression and is linked to poor prognosis in patients with breast cancer [23]. LYVE1, identified as a type I integral membrane glycoprotein, was associated with the promotion of ovarian tumor growth [24]. Which are consistent with our research. TMEM181 is a regulator of the Wnt signaling pathway, which plays an essential role in cell proliferation [25]. However, its role in OC remains elusive. KCTD20, implicated in non-small cell lung cancer progression, activated the FAK/AKT pathway and predicted poor prognosis [26]. VANGL1, whose expression varied in different cancers, its high expression has been correlated with a poor prognosis in patients with different cancers, including breast cancer, bladder cancer [27, 28]. Contrary to these findings, KCTD20 and VANGL1 were a protective factor in this study, suggesting diverse mechanisms across different cancer types. KCTD20 and VANGL1 may play a unique role in different cancer types. Furthermore, Kaplan-Meier survival analysis, risk score and ROC analysis collectively indicate that our model has a great predictive performance for OC (**Figure 5**).

The tumor microenvironment, intricate and dynamic, plays a pivotal role in tumor generation, progression and treatment resistance [29-31]. Tumor microenvironment scoring revealed that the high-risk group had a significantly higher stroma score, whereas the immune score was not significantly different (**Figure 6C**). Further analysis of immune cell infiltration showed that resting CD4 memory T cells, monocytes, activated mast cells, M0 macrophages, and naive B cells were positively linked to the risk score, whereas follicular helper T cells, CD8 T cells, activated CD4 memory T cells, activated NK cells, M1 macrophages, activated dendritic cells, and memory B cells were negatively linked to the risk score (Figure S1). These immune cells actively engage in both the development of the tumor immune microenvironment and tumor progression. Evidence has shown that these cells play a crucial role in OC. M1 macrophages produce pro-inflammatory factors and chemokines to exert

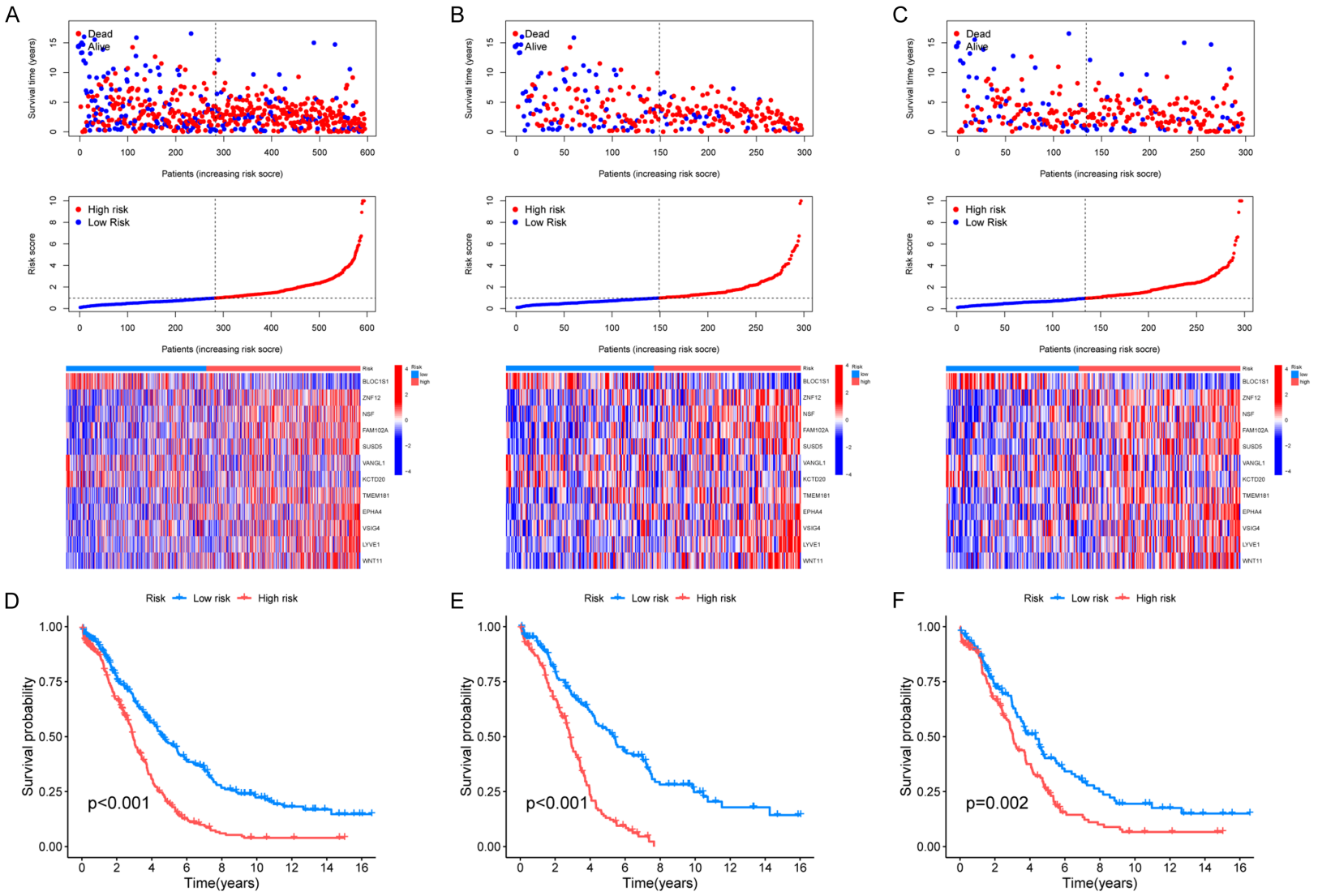
A
B
C
Dead
Alive
Survival time (years)
Patients (increasing risk socre)
High risk
Low Risk
Risk score
Risk
low
high
BLOC1S1
ZNF12
NSF
FAM102A
SUSD5
VANGL1
KCTD20
TMEM181
EPHA4
VSIG4
LYVE1
WNT11
D
E
F
Risk
Low risk
High risk
Survival probability
Time(years)
p<0.001
p<0.001
p=0.002

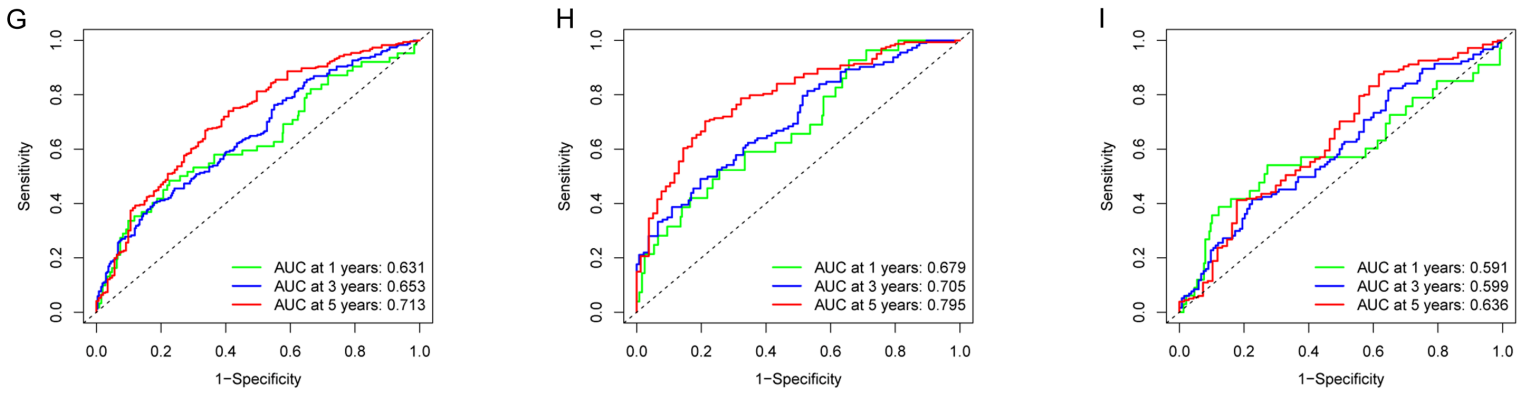

Figure 5. Evaluation of 3 cohort prognostic models. A-C. Risk point plots of survival time and survival status, distribution of risk scores, and heat maps of differential expression of prognostic genes between high- and low-risk groups for all, training and test cohorts. D-F. Kaplan-Meier curves for patients in the high-risk and low-risk groups in the all, training, and test cohorts. G-I. ROC curves display prognostic performance of the risk model in the all, training, and test cohorts.

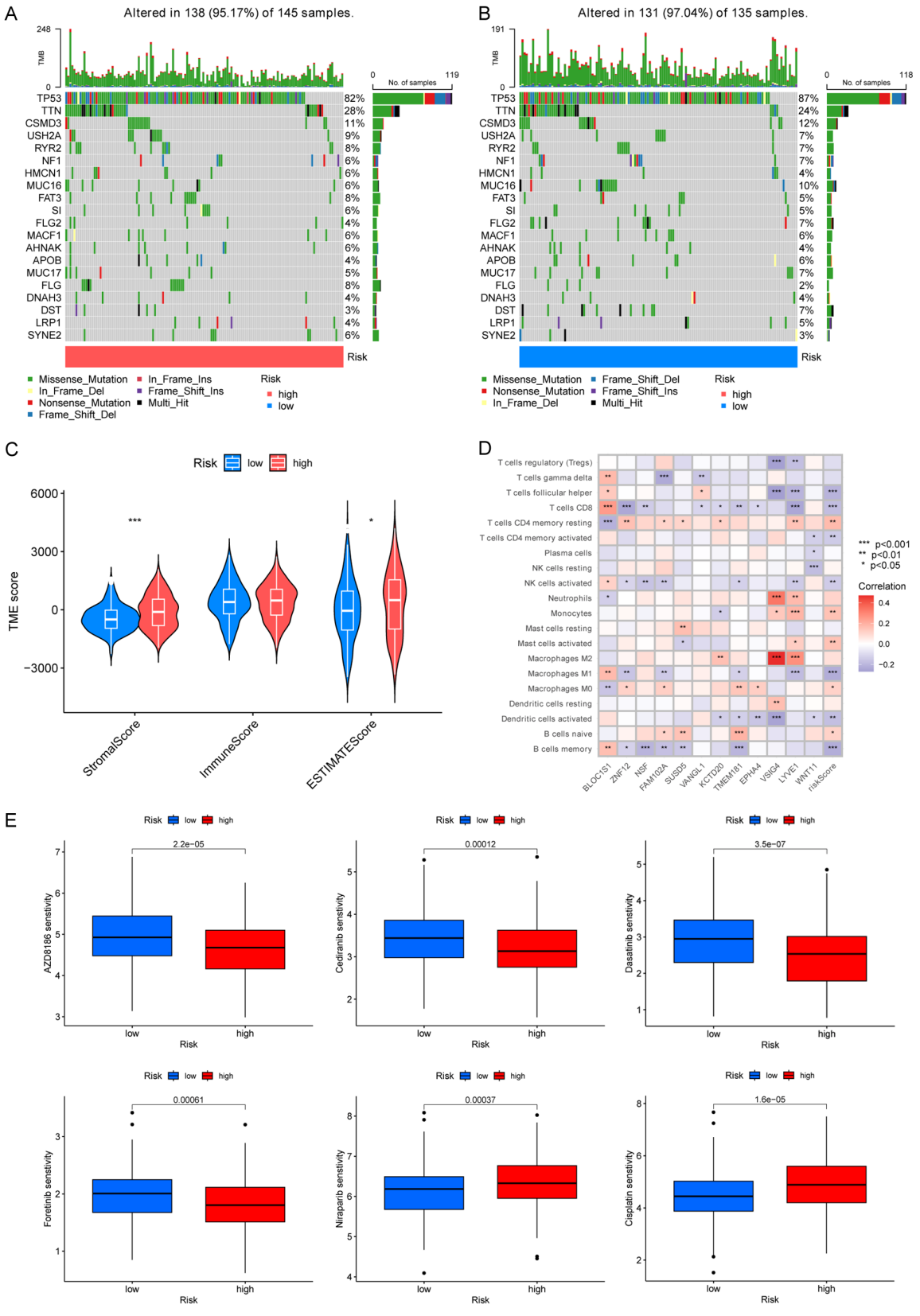

Figure 6. Correlation between risk score and TMB, TME score, immune cell infiltration, and drug sensitivity. A, B. Mutations of OC patients in high and low risk groups. C. Correlation between risk score and TME. D. Correlation between immune cells and 12 signature genes. E. Differences in chemotherapy sensitivity between high and low risk groups.

anti-tumor effects. While M2 macrophages have immunosuppressive effects, participate in angiogenesis and promote tumorigenesis and metastasis [32]. Notably, in OC, increased expression of M0 and M1 macrophages is strongly linked to a better prognosis, whereas increased expression of M2 macrophages is associated with an adverse prognosis [33]. The proportion of M1/M2 macrophages was higher in patients with low-grade OC compared with high-grade OC [34]. CD8 T cells play a critical role in eliminating cancer cells and exerting anti-tumor effects [35]. NK cells contribute to the elimination of circulating tumor cells, prevention of cancer metastasis, and participation in anti-tumor immunity [36]. Moreover, the correlation analysis between CTs prognostic signature genes and immune cell infiltration revealed that BLOC1S1 expression was positively correlated with CD8 T cells, M1 macrophages, suggesting that high expression of BLOC1S1 was accompanied by a corresponding increase in the content of CD8 T cells, M1 macrophages, which act as a protective factor and exert an anti-tumor effect, leading to a favorable prognosis for OC patients. VSIG4 and LYVE1 expressions correlated positively with M2 macrophages, neutrophils and monocytes, whereas ZNF12, NSF, FAM102A, TMEM181 and LYVE1 correlated negatively with NK cell activation (**Figure 6D**). Taken together, these findings suggest that the expression of these signature genes is associated with immune suppression in OC, consistent with previous analyses and suggesting a strong link between GTs and the formation and prognosis of the immunosuppressive microenvironment in OC.

In addition, patients with low- and high-risk scores showed significant differences in response to chemotherapy (**Figure 6E**). Niraparib is a PARP inhibitor that has been approved for the treatment of advanced OC patients with a high rate of recurrence with greater effectiveness and safety [37]. In our study, we discovered that patients with low-risk scores were more susceptive to the cisplatin and Niraparib, suggesting a higher response to treatment and better clinical outcomes. According to our findings, some of the commonly used anticancer drugs were more effective when they were used in high-risk patients, such as AZD8186, cediranib, dasatinib, and foretinib. Thus, predicting drug sensitivity in OC patients with different risks may provide new perspectives for the customization of personalized treatment approaches. Nevertheless, our research possesses certain limitations. The experimental data come from public databases. Consequently, it is inevitable that our results will be biased compared with the actual situation. Therefore, confirming the accuracy of our results through deeper investigation and experimental testing will be the direction of our future research.

Conclusion

In conclusion, with a comprehensive analysis of GTs in OC patients, we established a prognostic model for OC, and determined the validity of this prognostic risk model in predicting OC prognosis, tumor immune infiltration, and chemotherapeutic response. These findings provide a new perspective on OC prognosis and treatment, highlighting GTs as a promising therapeutic target for individuals with OC.

Disclosure of conflict of interest

None.

Address correspondence to: Yuting Liang, Center for Clinical Laboratory, The First Affiliated Hospital of Soochow University, Suzhou 215006, Jiangsu, The People's Republic of China. E-mail: liangyuting666@126.com

References

[1] Zhang R, Siu MKY, Ngan HYS and Chan KKL. Molecular biomarkers for the early detection of ovarian cancer. Int J Mol Sci 2022; 23: 12041.

[2] Sung H, Ferlay J, Siegel RL, Laversanne M, Soerjomataram I, Jemal A and Bray F. Global cancer statistics 2020: GLOBOCAN estimates of incidence and mortality worldwide for 36 cancers in 185 countries. CA Cancer J Clin 2021; 71: 209-249.

[3] Moufarrij S, Dandapani M, Arthofer E, Gomez S, Srivastava A, Lopez-Acevedo M, Villagra A and Chiappinelli KB. Epigenetic therapy for ovarian cancer: promise and progress. Clin Epigenetics 2019; 11: 7.

[4] Jayson GC, Kohn EC, Kitchener HC and Ledermann JA. Ovarian cancer. Lancet 2014; 384: 1376-1388.

[5] Ye Y, Dai Q, Li S, He J and Qi H. A novel defined risk signature of the ferroptosis-related genes for predicting the prognosis of ovarian cancer. Front Mol Biosci 2021; 8: 645845.

[6] Matulonis UA, Sood AK, Fallowfield L, Howitt BE, Sehouli J and Karlan BY. Ovarian cancer. Nat Rev Dis Primers 2016; 2: 16061.

[7] Eisenhauer EA. Real-world evidence in the treatment of ovarian cancer. Ann Oncol 2017; 28: viii61-viii65.
[8] Wu Y, Chen X, Wang S and Wang S. Advances in the relationship between glycosyltransferases and multidrug resistance in cancer. Clin Chim Acta 2019; 495: 417-421.
[9] Ohtsubo K and Marth JD. Glycosylation in cellular mechanisms of health and disease. Cell 2006; 126: 855-867.
[10] Haga Y and Ueda K. Glycosylation in cancer: its application as a biomarker and recent advances of analytical techniques. Glycoconj J 2022; 39: 303-313.
[11] Fernández LP, Sánchez-Martínez R, Vargas T, Herranz J, Martín-Hernández R, Mendiola M, Hardisson D, Reglero G, Feliu J, Redondo A and Ramírez de Molina A. The role of glycosyltransferase enzyme GCNT3 in colon and ovarian cancer prognosis and chemoresistance. Sci Rep 2018; 8: 8485.
[12] Li Y, Lin Y, Aye L, Dong L, Zhang C, Chen F, Liu Y, Fan J, Gao Q, Lu H, Lu C and Zhang S. An integrative pan-cancer analysis of the molecular and biological features of glycosyltransferases. Clin Transl Med 2022; 12: e872.
[13] Wilkerson MD and Hayes DN. ConsensusClusterPlus: a class discovery tool with confidence assessments and item tracking. Bioinformatics 2010; 26: 1572-1573.
[14] Yu G, Wang LG, Han Y and He QY. clusterProfiler: an R package for comparing biological themes among gene clusters. OMICS 2012; 16: 284-287.
[15] Hänzelmann S, Castelo R and Guinney J. GSVA: gene set variation analysis for microarray and RNA-seq data. BMC Bioinformatics 2013; 14: 7.
[16] Yoshihara K, Shahmoradgoli M, Martínez E, Vegesna R, Kim H, Torres-Garcia W, Treviño V, Shen H, Laird PW, Levine DA, Carter SL, Getz G, Stemke-Hale K, Mills GB and Verhaak RG. Inferring tumour purity and stromal and immune cell admixture from expression data. Nat Commun 2013; 4: 2612.
[17] Newman AM, Liu CL, Green MR, Gentles AJ, Feng W, Xu Y, Hoang CD, Diehn M and Alizadeh AA. Robust enumeration of cell subsets from tissue expression profiles. Nat Methods 2015; 12: 453-457.
[18] Liu B, Cheng L, Gao H, Zhang J, Dong Y, Gao W, Yuan S, Gong T and Huang W. The biology of VSIG4: implications for the treatment of immune-mediated inflammatory diseases and cancer. Cancer Lett 2023; 553: 215996.
[19] Liang L, Li J, Yu J, Liu J, Xiu L, Zeng J, Wang T, Li N and Wu L. Establishment and validation of a novel invasion-related gene signature for predicting the prognosis of ovarian cancer. Cancer Cell Int 2022; 22: 118.
[20] Xu J, Fang Y, Chen K, Li S, Tang S, Ren Y, Cen Y, Fei W, Zhang B, Shen Y and Lu W. Single-cell RNA sequencing reveals the tissue architecture in human high-grade serous ovarian cancer. Clin Cancer Res 2022; 28: 3590-3602.
[21] Kim J, Jung E, Ahn SS, Yeo H, Lee JY, Seo JK, Lee YH and Shin SY. WNT11 is a direct target of early growth response protein 1. BMB Rep 2020; 53: 628-633.
[22] Nie X, Liu H, Liu L, Wang YD and Chen WD. Emerging roles of Wnt ligands in human colorectal cancer. Front Oncol 2020; 10: 1341.
[23] Dong Y, Liu Y, Jiang A, Li R, Yin M and Wang Y. MicroRNA-335 suppresses the proliferation, migration, and invasion of breast cancer cells by targeting EphA4. Mol Cell Biochem 2018; 439: 95-104.
[24] Zhang N, Kim SH, Gainullina A, Erlich EC, Onufer EJ, Kim J, Czepielewski RS, Helmink BA, Dominguez JR, Saunders BT, Ding J, Williams JW, Jiang JX, Segal BH, Zinselmeyer BH, Randolph GJ and Kim KW. LYVE1+ macrophages of murine peritoneal mesothelium promote omentum-independent ovarian tumor growth. J Exp Med 2021; 218: e20210924.
[25] Zhang J, Yang X, Zhu S, Dai ZM and Zhu XJ. TMEM181: a key mediator of cytolethal distending toxin required for Wnt signaling activity. J Genet Genomics 2023; 50: 54-57.
[26] Zhang X, Zhou H, Cai L, Fan C, Liu Y, Wang L, Li Q and Miao Y. Kctd20 promotes the development of non-small cell lung cancer through activating Fak/AKT pathway and predicts poor overall survival of patients. Mol Carcinog 2017; 56: 2058-2065.
[27] Hatakeyama J, Wald JH, Printsev I, Ho HY and Carraway KL 3rd. Vangl1 and Vangl2: planar cell polarity components with a developing role in cancer. Endocr Relat Cancer 2014; 21: R345-356.
[28] Zhu J and Zhang F. Circular RNA VANGL1 knockdown suppressed viability, promoted apoptosis, and increased doxorubicin sensitivity through targeting miR-145-5p to regulate SOX4 in bladder cancer cells. Open Med (Wars) 2021; 16: 1010-1021.
[29] Xiao Y and Yu D. Tumor microenvironment as a therapeutic target in cancer. Pharmacol Ther 2021; 221: 107753.
[30] Arneth B. Tumor microenvironment. Medicina (Kaunas) 2019; 56: 15.
[31] Hinshaw DC and Shevde LA. The tumor microenvironment innately modulates cancer progression. Cancer Res 2019; 79: 4557-4566.
[32] An Y and Yang Q. Tumor-associated macrophage-targeted therapeutics in ovarian cancer. Int J Cancer 2021; 149: 21-30.
[33] Liu R, Hu R, Zeng Y, Zhang W and Zhou HH. Tumour immune cell infiltration and survival after platinum-based chemotherapy in high-

grade serous ovarian cancer subtypes: a gene expression-based computational study. EBioMedicine 2020; 51: 102602.

[34] Vankerckhoven A, Wouters R, Mathivet T, Ceusters J, Baert T, Van Hoylandt A, Gerhardt H, Vergote I and Coosemans A. Opposite macrophage polarization in different subsets of ovarian cancer: observation from a pilot study. Cells 2020; 9: 305.

[35] Reina-Campos M, Scharping NE and Goldrath AW. CD8(+) T cell metabolism in infection and cancer. Nat Rev Immunol 2021; 21: 718-738.

[36] Guillerey C. NK cells in the tumor microenvironment. Adv Exp Med Biol 2020; 1273: 69-90.

[37] González-Martín A, Pothuri B, Vergote I, DePont Christensen R, Graybill W, Mirza MR, McCormick C, Lorusso D, Hoskins P, Freyer G, Baumann K, Jardon K, Redondo A, Moore RG, Vulsteke C, O'Cearbhaill RE, Lund B, Backes F, Barretina-Ginesta P, Haggerty AF, Rubio-Pérez MJ, Shahin MS, Mangili G, Bradley WH, Bruchim I, Sun K, Malinowska IA, Li Y, Gupta D and Monk BJ; PRIMA/ENGOT-OV26/GOG-3012 Investigators. Niraparib in patients with newly diagnosed advanced ovarian cancer. N Engl J Med 2019; 381: 2391-2402.

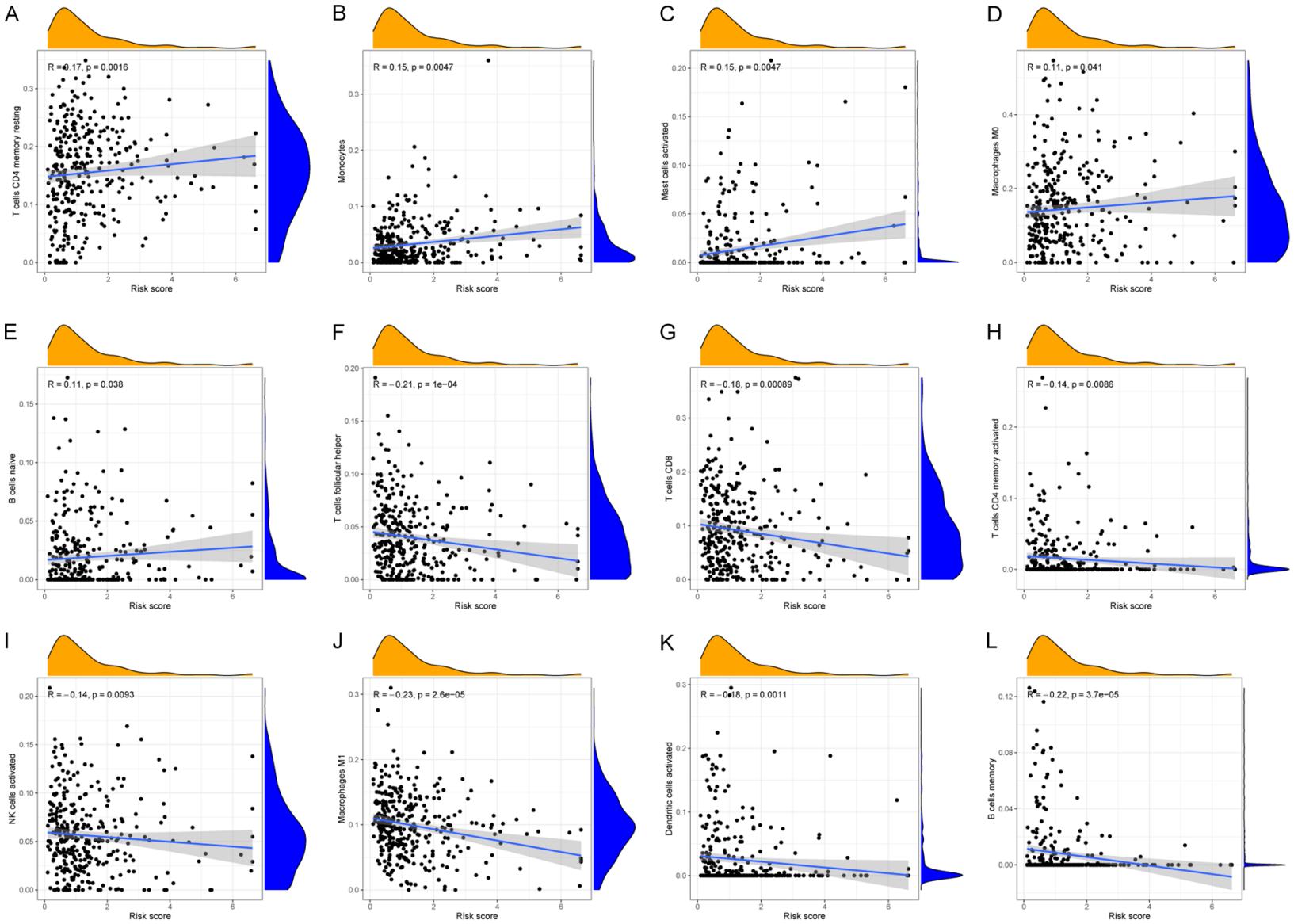

Figure S1. Correlation between immune cell and risk score. A-L. Resting CD4 memory T cells, monocytes, activated mast cells, M0 macrophages, naive B cells, follicular helper T cells, CD8 T cells, activated CD4 memory T cells, activated NK cells, M1 macrophages, activated dendritic cells, and memory B cells.